1

Clay Mineral Nanotubes: Stability, Structure and Properties

Hélio A. Duarte[1], Maicon P. Lourenço[1],
Thomas Heine[2] and Luciana Guimarães[3]
[1]*Department of Chemistry, ICEx,*
Universidade Federal de Minas Gerais, Belo Horizonte, MG,
[2]*School of Engineering and Science, Jacobs University Bremen, Bremen,*
[3]*Department of Natural Science, Universidade Federal de São João Del Rei,*
São João Del Rei, MG
[1,3]*Brazil,*
[2]*Germany*

1. Introduction

Recent developments in nanoscience and nanotechnology opened fundamental and applied new frontiers in science and materials engineering. Advanced materials are being developed with enhanced chemical and physical properties with unique characteristics. The properties of these materials are determined not only by their composition and chemical bonds, but also by size and morphology.

The emerging field of nanotechnology is mostly focused on carbon and inorganic based nanomaterials, such as carbon nanotubes, graphene, transition metal nanotubes and nanowires (Iijima, 1991; Tenne *et al.*, 1992; Endo *et al.*, 1996; Dresselhaus *et al.*, 2001). Systems containing aluminosilicates have been investigated as mesoporous materials in the form of zeolite and alumina. Although they have not yet received as much attention, clay minerals can also form nanostructured layered materials and nanotubes with remarkable geometric properties. Imogolite is the most representative species of this case, since it has been studied in a pre-nano (1970) decade (Cradwick *et al.*, 1972) and has been nearly forgotten until recently. Since 2000 (Bursill *et al.*, 2000; Tamura & Kawamura, 2002; Mukherjee *et al.*, 2005; Nakagaki & Wypych, 2007), these structures gained again prominence in the literature and appear as an emerging field of research. They can be used as nanoreactors for selective catalysts, adsorbent, nanocable, support for the immobilization of metalloporphyrins, encapsulation and ionic conductor (Nakagaki & Wypych, 2007; Kuc & Heine, 2009).

Although the nanotube (NT) term is recent, the idea of a small tubular structure is not new. In 1930, Linus Pauling (1930) proposed the existence of cylindrical structures formed by minerals in nature. Based on asbestos related minerals, Pauling proposed that if two faces of a mineral are not symmetrical, there will be a structural mismatch between the layers leading to its deformation and curvature. Chrysotile, halloysite and imogolite are examples of such structures. Unfortunately, Pauling concluded that layered materials with symmetric

structure, such as WS_2 and MoS_2, are not likely to form closed cylindrical structures. It took, however, until 1992 when Tenne, Remskar and others showed that tubular structures are possible from these materials regardless of the missing symmetry (Tenne *et al.*, 1992; Remskar, 2004; Tenne, 2006).

Imogolite, Halloysite, and Chrysotile are examples of naturally occurring nanostructured clay minerals. Imogolite occurs naturally in soils of volcanic origin and is composed of single-walled NTs. The tube walls consist of a curved gibbsite-like sheet ($Al(OH)_3$), where the inner hydroxyl surface of the gibbsite is substituted by (SiO_3)OH groups. This structure possesses a composition of $(HO)_3Al_2O_3SiOH$, which is the sequence of atoms encountered on passing from the outer to the inner surface of the tube (Guimaraes *et al.*, 2007). Halloysite is a clay mineral with stoichiometry $Al_2Si_2O_5(OH)_4 .nH_2O$ that can grow into long tubules and is chemically similar to kaolinite (Giese & Datta, 1973; White *et al.*, 2009). It consists of a gibbsite octahedral sheet ($Al(OH)_3$), which is modified by siloxane groups at the outer surface (Guimaraes *et al.*, 2010). The chrysotile structure is composed of brucite ($Mg(OH)_2$) and tridymite (silicon dioxide, SiO_2) layers. The brucite octahedral sheet forms the outer side of the tube and SiO_4 groups are anchored to the inner side of the tube (Piperno *et al.*, 2007).

The structures of imogolite (Cradwick *et al.*, 1972), halloysite (Bates *et al.*, 1950a) and chrysotile (Bates *et al.*, 1950b) have been identified between the 1950th and 1970ths through spectroscopic methods. However, recently, those clays again became the focus of research and patents (Price & Gaber; Redlinger & Corkery, 2007) due to the great interest in the nanometric structures. Nanostructures (nanotubes and nanospirals) of clay minerals are very versatile systems, and are target materials for applications in catalysis (Imamura *et al.*, 1996), molecular sieves and adsorbents (Ackerman *et al.*, 1993), inorganic support for catalysts (Nakagaki & Wypych, 2007), controlled drug release (Veerabadran *et al.*, 2007), formation of composites, controlled release devices of herbicides, fungicides and insecticides (Lvov *et al.*, 2008) and anti-corrosion agents.

The increasing interest of clay mineral based NTs requires better understanding of their structures and properties. However, in most cases, samples of natural and synthetic compounds present only low crystallinity, leading to low-resolution structural data from X-ray diffraction measurements. Thus, a complementary approach involving spectroscopic methods and computational simulation can help in the interpretation of results and obtained structural data.

In the present chapter, the stability and properties of the nanostructured aluminosilicates will be reviewed and discussed with the focus on the computer modeling of such systems. The first theoretical investigations on the aluminosilicate NTs were mostly based on force fields specially developed for these systems (Tamura & Kawamura, 2002). The size of the unit cell is normally a limitation for using quantum mechanical calculations. Notwithstanding, quantum mechanical methods are being applied to such systems. Density functional theory (DFT), presently the most popular method to perform quantum-mechanical calculations, is the state-of-the-art method to study clay mineral nanotubes with high predictive power. First applications used the approximation to DFT implemented to the SIESTA (Artacho *et al.*, 1999; Soler *et al.*, 2002) code, which uses pseudo potentials and localized numerical atomic-orbital basis sets and it is well parallelized for multicore machines. Recently, the helical symmetry has been implemented in the CRYSTAL (Dovesi *et*

al., 2009) program, reducing significantly the computational costs for treating high-symmetry nanotubes (those at the equilibrium position in case no Peierls distortions are present), and hence making full-electron calculations of these systems feasible. However, if one investigates chemical modification in the NT structure, the use of helical symmetry becomes limited. In the last few years we have used an approximate Density Functional method called Density Functional based Tight Binding with self Consistent Charge corrections (SCC-DFTB) (Elstner *et al*., 1998) method, as implemented in the deMon-nano (Heine *et al*., 2009) and DFTB+ programs (Aradi *et al*., 2007). The SCC-DFTB method, for a recent review see (Oliveira *et al*., 2009), can lead to results which are nearly equivalent to DFT calculations although some orders of magnitude faster. The SCC-DFTB method uses a non-orthogonal tight-binding approach where all parameters are consistently computed using DFT, together with a minimal valence basis set. This method has been successfully applied to inorganic and carbon NTs (Enyashin & Seifert, 2005; Ivanovskaya *et al*., 2006; Stefanov *et al*., 2008; Enyashin *et al*., 2009; Kuc & Heine, 2009; Rasche *et al*., 2010). In our laboratory, we have applied successfully the SCC-DFTB method to investigate the stability, electronic and mechanical properties of the nanostructured aluminosilicates (Guimaraes *et al*., 2007; Kuc & Heine, 2009; Guimaraes *et al*., 2010).

2. Imogolite-like nanotubes – Gibbsite as a template for new materials

The careful analysis of the imogolite structure is particularly elucidative and can help to envisage strategies to design new materials. It is normally described as a NT where the external part consists of a curved gibbsite-like sheet ($Al(OH)_3$ and in the inner hydroxyls are replaced by $SiO_3(OH)$ groups.

The gibbsite structure (figure 1a) is a layered material with the $Al(OH)_3$ stoichiometry. Normally it crystallizes in hexagonal or prismatic structures with monoclinic symmetry. Each sheet of gibbsite is composed by hexacoordinated aluminum atoms arranged between two layers of hydroxyls. Each hydroxyl bounds to two aluminum centers, resulting in electrically neutral sheets. The layers are kept together through hydrogen bonds.

The hypothetical gibbsite monolayer (Frenzel *et al*., 2005) and the respective gibbsite NT (Enyashin & Ivanovskii, 2008) have been investigated using DFT and SCC-DFTB calculations. The strain energy, that is, the relative energy with respect to the planar monolayer, depicted in figure 2, does not show a minimum. It presents the same behavior as other inorganic and carbon NTs (Enyashin *et al*., 2007). However, the hypothetical gibbsite NT is unlikely to be synthesized using conventional synthesis approaches in aqueous solution through hydrolysis, as this is leading to the thermodynamic most stable lamellar structure. It is important to point out that other inorganic and carbon NTs are synthesized in very specific and well controlled experiments and the NTs are the kinetic product of the synthesis. It is well known that graphene is equivalent to a nanotube with infinite diameter and represents the more stable conformation with respect to the carbon NTs.

Figure 1b shows clearly how the fragment SiO_4^{4-} binds to the gibbsite surface to form imogolite. The mismatch of the bond lengths lead to the curvature of the gibbsite layer and to the formation of the imogolite NT. There is an optimal curvature which leads to the minimum strain in the structure. This explains why imogolite is monodisperse with very well-defined geometrical parameters and symmetry.

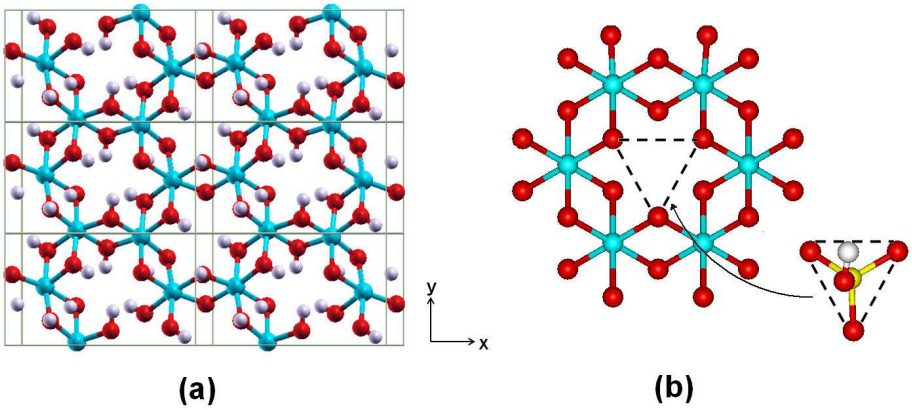

Fig. 1. a) Periodic gibbsite layer model. b) Hexagonal gibbsite ring where silanol is bound.

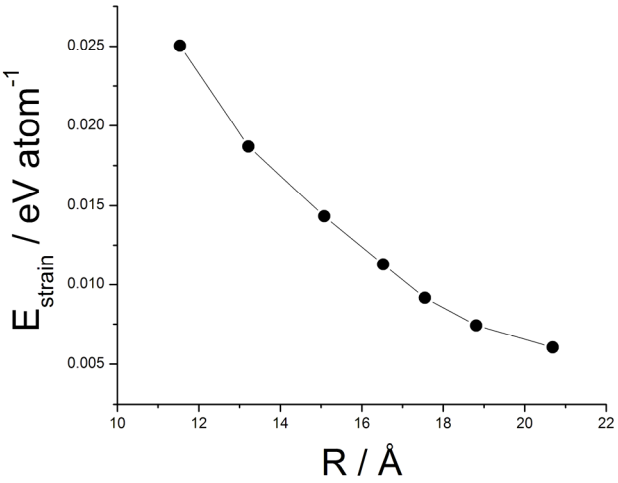

Fig. 2. Calculated strain energies E_{str} as a function of the radius R for zigzag hypothetical gibbsite NTs.

The roll-up process can lead to different symmetries depending on the rolling direction **B** in the 2D lattice (figure 3-a), where $\mathbf{B}=n\mathbf{a_1}+m\mathbf{a_2}$ ($\mathbf{a_1}$, $\mathbf{a_2}$ are lattice vectors of the hexagonal lattice). In principle, three classes of NTs can be constructed: *armchair* (*n,n*), *zigzag* (*n,0*) and "*chiral*" (*n,m*), with $n \neq m$. However, only *zigzag* tubes (figure 3-b) have been experimentally observed.

The synthesis of imogolite occurs in mild conditions and in aqueous solution. However, its mechanism of formation is rather complex and involves self assembly. The Al^{3+} ions in solution rapidly hydrolyze forming polynuclear species (Bi *et al.*, 2004). It has been pointed out that the thermodynamic equilibrium is not achieved rapidly and the kinetics is very slow (Casey, 2006). The silicates in solution are a very complicated system forming many polynuclear intermediates (Exley *et al.*, 2002; Schneider *et al.*, 2004). The imogolite formation

mechanism may occur through self assembly, where silicate and aluminate species are combined to form proto-imogolite. It is important to highlight that this process is very sensitive to pH, ionic strength and concentration. The many concurrent reaction channels can be displaced very easily modifying the equilibria and the product. In fact, it is well known that the pH has to be tightly controlled in order to successfully synthesize imogolite. In fact, only recently, it has been shown that the imogolite formation mechanism involves proto-imogolite structures which oligomerize to form the NTs (Doucet *et al.*, 2001; Mukherjee *et al.*, 2005; Yucelen *et al.*, 2011). The fact that the synthesis occurs in aqueous solution means that the pH and, consequently, the involved species acidic constants (pKa=-log(Ka)) are very important and guide the hydrolysis.

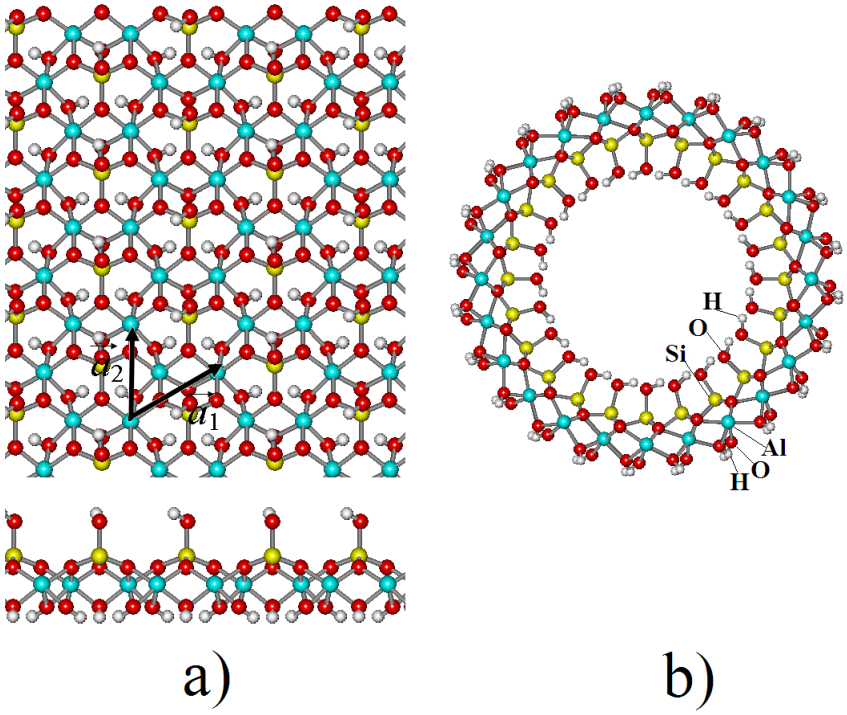

Fig. 3. (a) Hypothetical 2D imogolite layer with vector a_1 and a_2 and (b) *zigzag* (12,0) imogolite NT. White atoms, H; red, O; gray, Al; yellow, Si. Adapted with permission from (Guimaraes *et al.*, 2007). Copyright 2007 American Chemical Society.

Recently, the imogolite-like structure aluminogermanate has been synthesized (Levard *et al.*, 2008; Levard *et al.*, 2010). Here, the SiO_4^{4-} is replaced by GeO_4^{4-} fragments. However, to the best of our knowledge, no other imogolite-like structure except Ge-imogolite has been synthesized so far. Species such as H_3PO_4, H_3AsO_3, H_3AsO_4 are also strong candidates to form imogolite-like structures. However, it seems that their acid/base properties would lead to drastically different experimental conditions in order to perform the synthesis. The experimental conditions for synthesizing other imogolite-like NTs remain to be determined.

In table 1, the pKa of the different species are presented. $Ge(OH)_4$ and $Si(OH)_4$ have similar pKa values, possibly explaining why the alumino-germanate NTs have been synthesized using similar procedures. Comparing the pKa values of the species at table 1, one could argue that aluminoarsenite NTs also could be synthesized in similar experimental conditions of the aluminosilicate NTs, while for NT based on phosphoric and arsenic acid it would be necessary to decrease the pH. Although the synthesis of imogolite-like structures is very challenging, it is an interesting strategy for designing new nanostructured materials. Replacing the $Si(OH)_4$ species in the imogolite structure, one can easily control the diameter and electrostatic potential of the NT inner part.

Finally, gibbsite can be envisaged as a template for developing new nanostructured materials such as imogolite-like NTs. The mild conditions for the synthesis in aqueous solutions make them very attractive for technological and environmental applications.

Species	Distance / Å		pKa
	M-O	O-O	
$[Al(H_2O)_6]^{3+}$	1.934	-	5.52
$Si(OH)_4$	1.663	2.665	9.84
$Ge(OH)_4$	1.799	2.877	9.16
H_3PO_4	1.473/1.641[2]	2.619	2.12/7.21/12.67
H_3AsO_4	1.615/1.811[2]	2.869	2.19/6.94/11.5
H_3AsO_3	1.839	2.841	9.2

Table 1. Acidity constants and geometrical parameters of species. Calculations performed at the PBE/TZVP level of theory; Distances related to double and single bonds, respectively.

3. Imogolite nanotubes – Stability and structural properties

It is still an unsolved problem controlling the dimensions of nanotubes during synthesis in order to produce monodisperse NTs. Several theoretical studies on NTs, such as C, BN, MoS_2, TiO_2 (Hernandez *et al.*, 1998; Seifert *et al.*, 2000; Enyashin & Seifert, 2005) have shown that the strain energy decreases monotonically with increasing of tube radius. No energy minimum is observed in the strain energy curve. Therefore, these NTs are not thermodynamical products and they must be seen as kinetic products.

However, as shown elsewhere (Mukherjee *et al.*, 2005; Yucelen *et al.*, 2011), dealing with a number of experimental conditions (e.g., reactant composition, concentration, pH, temperature and time) it is possible to control structure, dimensions and composition of aluminosilicate (imogolite) and aluminogermanate NTs. Imogolite NTs are single walled and present well defined structure and dimensions. The external and internal diameters of imogolite NTs are estimated to be 2.3 and 1.0 nm, respectively, with average length of 100 nm.

At present, the stability of imogolite NTs is well investigated. Several theoretical studies (Tamura & Kawamura, 2002; Konduri *et al.*, 2006; Alvarez-Ramirez, 2007; Guimaraes *et al.*, 2007; Zhao *et al.*, 2009; Demichelis *et al.*, 2010; Lee *et al.*, 2011) using different methodologies indicated that there is clearly a minimum in the strain energy curve of the imogolite. However, the minimum value is still a matter of controversy. In 1972, based on X-ray and

electron diffraction analyses, Cradwick et al. (1972) first reported that the circumference of natural imogolite NT is composed by 10 hexagonal gibbsite rings. Few years later, Farmer et al. (1977) have synthesized the first imogolite nanotube which contained 12 hexagonal gibbsite rings around its circumference, figure 3.

The first theoretical assessment on NT stability was carried out in the framework of molecular dynamics simulation using a classical many-body potential (Tamura & Kawamura, 2002) with specific parameters for imogolite. The total energy obtained with this method has the minimum strain energy per atom around a tube diameter of 2.6-2.9 nm, which means 16 gibbsite units around the circumference. Konduri et al. carried out molecular dynamics simulations for imogolite NTs employing the CLAYFF force field (Konduri *et al.*, 2006). According to this work, the force field accurately reproduced the properties of aluminosilicate minerals including gibbsite, and the CLAYFF simulations (Konduri *et al.*, 2006) reproduced the experimental findings of Farmer et al. (1977) with 12 gibbsite units around the tube.

The *zigzag* and *armchair* imogolite NTs stabilities have been studied within SCC-DFTB by (Guimaraes *et al.*, 2007). The calculated strain energy per atom for both chiralities have shown the same behavior, although *zigzag* NTs are more stable than *armchair* ones and have a minimum with 12 gibbsite units around circumference, i.e., (12,0) (figure 4).

The NT stability can also be explained in the framework of a model based on the classical theory of elasticity. For several NTs, including C, BN, MoS_2, TiO_2 (Hernandez *et al.*, 1998; Seifert *et al.*, 2000; Enyashin & Seifert, 2005) the tube's strain energy E_{str} per atom can be related to the elastic modulus Y, the thickness h of monolayer and by the tube radius R:

$$E_{str} = \frac{a}{R^2} \sim \frac{Yh^3}{R^2} \tag{1}$$

The strain energy per atom follows the general trend $1/R^2$ for all known NTs except for imogolite. When the tube is formed by a symmetric layer, equation 1 is valid. Imogolite is composed of nonsymmetrical aluminosilicate layer and a difference in the surface tensions $\Delta\sigma$ of outer and inner tube surfaces must be taken into account. As a result, an additional contribution is included to strain energy as can be seen in equation 2 and 3.

$$E_{str} = \frac{a}{R^2} + \frac{b}{R} \sim \frac{Yh^3}{R^2} + \frac{\Delta\sigma \cdot h}{R} \tag{2}$$

$$E_{str} = \frac{5.2}{R^2} - \frac{1.1}{R} \tag{3}$$

In which E_{str} is given in eV atom^{-1}, R in Å, $\boldsymbol{a}$ in eV atom^{-1} Å^2, and $\boldsymbol{b}$ in eV atom^{-1} Å. The surface energy $\Delta\sigma$ supports a negative curvature, which decreases the strain energy and introduces a minimum into the $E_{str}(R)$ curve. The fit of the obtained E_{str} and R values for imogolite NTs using equation 2 describes the change of the strain energy in the wide range of radii quite well (figure 4).

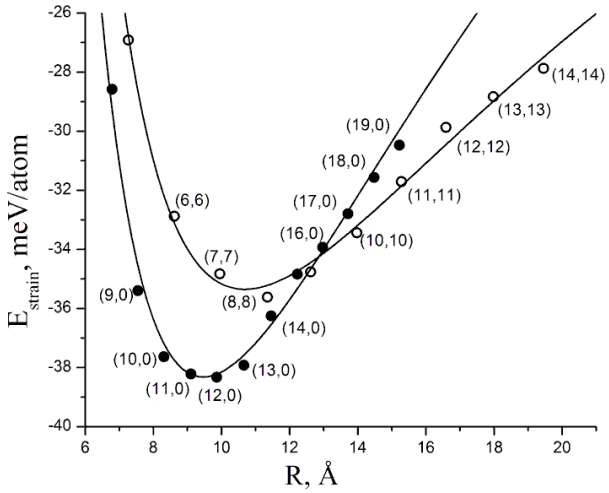

Fig. 4. Calculated strain energies E_{str} as a function of the radius R for *zigzag* (closed circles) and *armchair* (*open circles*) imogolite NTs. Reprinted with permission from (Guimaraes *et al.*, 2007).Copyright 2007 American Chemical Society.

First-principles calculations based on density functional theory (DFT) have been performed to study the energetics of imogolite NT as a function of tube diameter (Zhao *et al.*, 2009). A localized linear combination of numerical atomic-orbital basis sets has been used for the valence electrons and nonlocal pseudopotentials have been adopted for the atomic core. The DFT strain energy curve for imogolite NTs indicates an energy minimum for (9,0) structure. Furthermore, there is a local energy minimum for (12,0) nanotube, being 0.14 kJ mol^{-1} less stable than (9,0) structure. The authors assign both global and local energy minima as the natural and synthetic imogolite NTs. According to them, due to the curvature effect of the NTs, the energy minimum arises from shortening of Al-O and Si-O in the inner wall and increase of Al-O bonds in the outer wall.

Recently, first-principles calculations based on DFT have also been performed in order to study the origin of the strain energy minimum in imogolite NTs (Lee *et al.*, 2011). Although the same methodology (DFT), functional (PBE), local basis and program (SIESTA) had been used as the previous discussed work (Zhao *et al.*, 2009), the strain energy curve profile and minimum for imogolite are different. Lee et al. (2011) have found a minimum at (8,0) and the strain energy curve does not present any local minimum, in contrast to Zhao et al. (2009) that found the most stable structure at (9,0) and a local minimum at (12,0).

Demichelis *et al.* (2010) also contributed to the imogolite energy minimum topic. The authors explored the structure and energetics of imogolite NTs in the framework of full electron DFT. In contrast to the previously discussed works mentioned so far, Demichelis *et al. (*2010) have used a hybrid functional (B3LYP) in the CRYSTAL program, without the usage of parameterized pseudo potentials (Demichelis *et al.*, 2010). The obtained total energy curve presents a well defined minimum at (10,0) for zigzag NTs and (8,8) for armchair. In order to closely compare the results with ones obtained by Zhao *et al.* (2009), Demichelis *et al.* (2010) have optimized the most stable imogolite structures (n=8-13) using the PBE

exchange-correlation functional. The total energy curve presents a minimum at (9,0), in contrast to (10,0) from B3LYP, although the absolute energy difference is only 0.4 kJ mol^{-1} per formula unit. Besides, Demichelis *et al.* (2010) have assigned the reason imogolite *zigzag* NTs (*n*,0) are more stable than *armchair* (*n*,*n*), which are mainly related to the geometrical setting of the inner wall. According to Demichelis *et al.* (2010), oxygen atoms from neighboring SiO_4 present shorter distances for (n,0) tubes compared to (*n*,*n*). Moreover, the presence of hydrogen bonds chains in the inner wall of the zigzag tubes allows stabilization of the curled structure in comparison to the armchair one. Lee *et al.* (2011) also presented evidences that the unique arrangement of inner silanol groups (Si-OH) and the hydrogen network are the origin of the strain energy minimum and are the reason for preference of the zigzag chirality. According to those authors, depending on the rolling direction, inner silanol OH groups produce distinct hydrogen bond (HB) networks, e.g., for *zigzag* tubes occurs disk inner HB because inner OH groups are aligned with zigzag like rolling direction in parallel and helix-like inner HB networks occurs to armchair. The *zigzag* NTs can effectively construct inner HB networks. In order to evaluate the *zigzag* preference, Lee *et al.* (2011) have investigated the structural relaxation of hydrogen saturated curved gibbsite-like imogolite, i.e., a piece of gibbsite like with armchair configuration. The obtained results have shown the curved gibbsite-like tubes spontaneously change the chirality from armchair to zigzag by shortening inner HB distances and changing the rolling direction. However, it is important to note that for all discussed works the calculations have been performed in the gas phase and it does not take into account the water solvent and the rather large interaction of the protons with the solvent. Furthermore, the synthesis of imogolite is carried out in aqueous solution and the water must play an important role in the HB network formed inside and outside the imogolite NT.

Besides the structural properties, the electronic and mechanical properties of imogolite NTs have also been calculated. For instance, from SCC-DFTB (Guimaraes *et al.*, 2007) estimates, imogolite is insulator with high band gap value. The calculated Young's moduli for imogolite lies in the range of 175-390 GPa, similar to the other inorganic NTs such as MoS_2 (230 GPa) and GaS (270 GPa). The electrostatic field based on the SCC-DFTB charges is shown at figure 5. Imogolite presents negative charges at the inner walls and positive charges at the outer walls. However, it is important to note that these are gas phase calculations and in the aqueous solution the acidity of the hydroxyl groups can change the charge distribution along the structure.

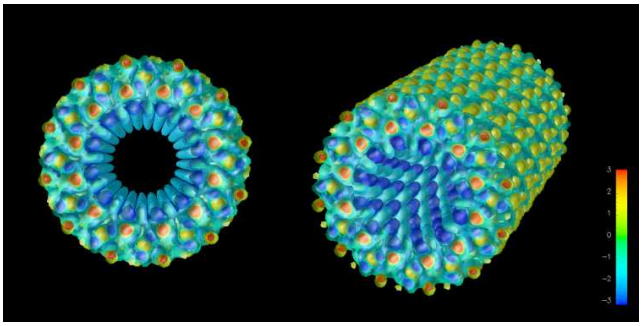

Fig. 5. Electrostatic field of the imogolite (12,0). Adaptedwith permission from (Guimaraes *et al.*, 2007). Copyright 2007 American Chemical Society.

4. Halloysite nanotubes – Stability and structural properties

Halloysite is a clay mineral normally described as a gibbsite octahedral sheet ($Al(OH)_3$), which is modified by siloxane groups at the outer surface (figure 6), and has a 1:1 Al:Si ratio and stoichiometry $Al_2Si_2O_5(OH)_4.nH_2O$ (Guimaraes *et al.*, 2010). Halloysite exhibits a range of morphologies, and according to Joussein *et al.* (2005) the structure will depend on crystallization conditions and geological occurrences. Various morphologies are reported in the literature, as platy and spheroidal crystals, scroll, glomerular or 'onion-like' and the hollow tubular structure, which is the most common one. The size of halloysite tubes varies from 500-1000 nm in length, 15-100 nm in inner diameter, depending on the substrate (Guimaraes *et al.*, 2010).

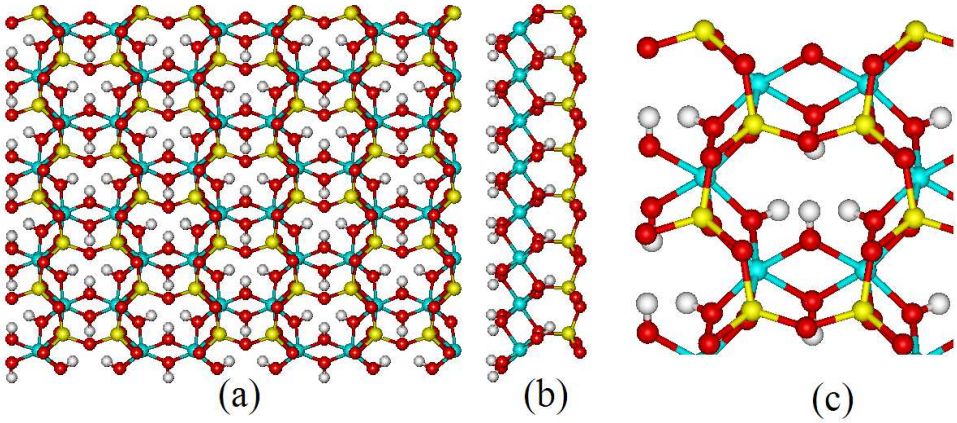

Fig. 6. Halloysite layer formed by gibbsite octahedral sheet and siloxane groups. (a) top view and (b) side view. (c) Detail of the top view. White atoms are H, red - O, blue – Al, yellow – Si.

Halloysite has the same stoichiometrical composition of kaolinite, except for its water content. Layered halloysite occurs mainly in two different polymorphs, the hydrated form (with interlayer spacing of 10 Å) with the formula $Al_2Si_2O_5(OH)_4.2H_2O$ and the anhydrous form (with interlayer spacing of 7 Å) and kaolinite composition - $Al_2Si_2O_5(OH)_4$. The intercalated water is weakly bound and can be readily and irreversibly removed (Joussein *et al.*, 2005).

According to Lvov *et al.* (2008) the reason why planar kaolinite rolls into a tube remains unclear. In the review article of Joussein *et al.* (2005) some questions are pointed out. Dixon and Mckee (Dixon & McKee, 1974) proposed the tubes are formed by layer rolling, caused by dimensional mismatch between the octahedral and tetrahedral layers and weak interaction bonds. In the hydrated halloysite, the rolling leaves a small space between the adjacent layers, although the dehydration does not change the structure. As reported by Bailey (1990) the dimensional mismatch between the octahedral and tetrahedral layers also occurs to kaolinite. However, the mismatch is corrected by rotation of alternate tetrahedral in opposite directions, while in halloysite the rotation is blocked by interlayer water molecules.

Halloysite NTs are attractive materials due to availability and vast range of applications. Besides, in contrast to other nanomaterials, naturally occurring halloysite is easily obtained and an inexpensive nanoscale container. For instance, halloysite is a viable nanocage for inclusion of biologically active molecules with specific sizes due to the empty space inside the NT (Price & Gaber; Price *et al.*, 2001). It has been used as support for immobilization of catalysts such as metallocomplexes (Nakagaki & Wypych, 2007; Machado *et al.*, 2008) and for the controlled release of anti-corrosion agents, herbicides, fungicides (Price & Gaber; Shchukin *et al.*, 2006; Shchukin & Mohwald, 2007). It exhibits interesting features and offers potential application as entrapment of hydrophilic and lipophilic active agents, as enzymatic nanoscale reactor (Shchukin *et al.*, 2005); as sustained release of drugs (Price *et al.*, 2001; Levis & Deasy, 2003; Kelly *et al.*, 2004; Veerabadran *et al.*, 2007); as adsorbing agent for dye removal (Liu *et al.*, 2011). It can be employed to improve mechanical performance of cements and polymers (Hedicke-Höchstötter *et al.*, 2009).

Imogolite and halloysite have the same gibbsite layer composition but differ in the arrangement of silicate atoms and in the Al:Si ratio, 2:1 and 1:1, respectively. The way silicon atoms are bonded to gibbsite octahedral rings is also different. In imogolite NT, $(SiO_3)OH$ groups are anchored to the inner side of the tube at gibbsite octahedral rings (figure 7a), while in halloysite siloxane groups are bonded via only one oxygen atom to gibbsite octahedral rings at the outer part (figure 7b), and the apical oxygen of tetrahedra becomes the vertices of octahedra.

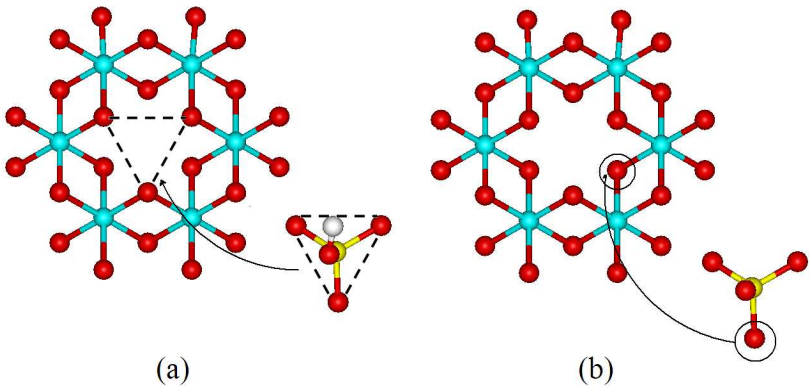

Fig. 7. Scheme presenting the different way silicon atoms are bonded to gibbsite octahedral ring at (a) imogolite and (b) halloysite.

As discussed earlier, the strain energy of imogolite NTs is an apparent exception, once instead of decreasing monotonically this function presents a minimum. At a first glance, the strain energy per atom for halloysite NTs (figure 8) decreases with increasing tube radius (R) and converges approximately as $1/R^2$, as demonstrated with SCC-DFTB calculations (Guimaraes *et al.*, 2010). However, a detailed look at the calculated values E_{str} shows that they can be better fitted by the following equation (Eq. 4):

$$E_{str} = \frac{49.0}{R^2} - \frac{3.0}{R} \tag{4}$$

In which E_{str} is given in eV atom^{-1} and R in Å. The values of 49.0 and 3.0 are given in eV atom^{-1} Å^2 and eV atom^{-1} Å, respectively. For a wide region between 24 and 54 Å of the extrapolated curve, halloysite NTs have slightly negative values for strain energies and are more stable than the respective monolayer. Thus, halloysite NTs are described by a similar equation used to fit the strain energies of imogolite NTs (Guimaraes *et al.*, 2007). It is not an unexpected result, since halloysite NTs are composed of an asymmetrical aluminosilicate layers and should have different tension promoting the formation of a curved structure.

The minimum of E_{str} curve for halloysite NTs is much less pronounced compared to that of imogolite NTs, the minimum is only 7 meV/atom below the energy of the layer, which is 5-6 times smaller than the corresponding values for imogolite. This explains the morphological distinction between experimental observations on halloysite and imogolite, that exist as multi-walled and single-walled NTs, respectively. The strain energy difference between halloysite NTs is small enough to explain the existence of a set of multi-walled NTs with large radii distribution. In contrast, imogolite NTs are strongly monodisperse.

Halloysite is an aluminosilicate which has two different basal faces. The first one consists of a tetrahedral silicate surface Si-O-Si while the other basal surface has gibbsite octahedral layer ($Al(OH)_3$). In principle, both faces are – as ideal structures in theory - electrically neutral. The charges inside and outside halloysite NTs are related to their structure and adsorption properties. The charges obtained with SCC-DFTB calculations (Guimaraes *et al.*, 2010) have been used to get the electrostatic potential map of some halloysite NTs, as shown in figure 9. As it can be seen, the inner wall of tube is mainly positively charged, while the outer surface has a weakly negative charge, in good agreement with observations by Lvov *et al.* (2008). According to these authors, below pH 8.5 the tube cavity has a positive inner surface and negatively charged outer surface.

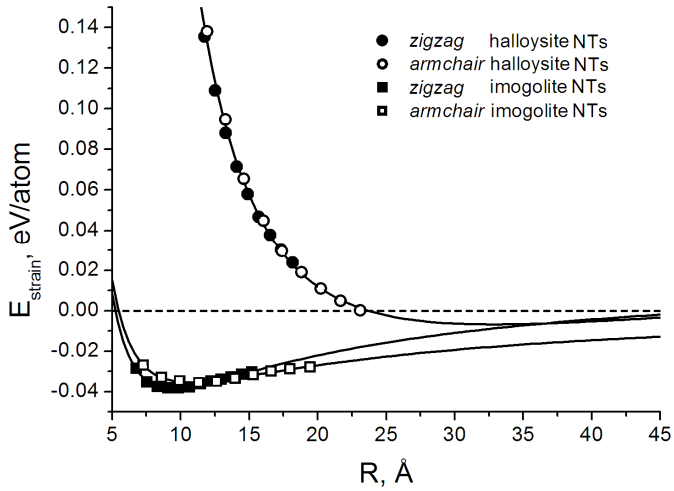

Fig. 8. Strain energy as a function of tube radius for (*n,0*) (closed circles) and (*n,n*) (open circles) single walled halloysite NTs and (*n,0*) (closed squares) and (*n,n*) (open squares) single walled imogolite NTs. Reprinted with permission from (Guimaraes *et al.*, 2010) Copyright 2010 American Chemical Society.

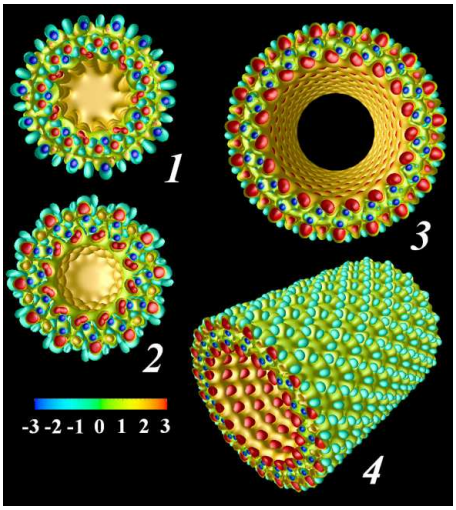

Fig. 9. Electrostatic field nearby halloysite NTs of different chiralities:
1 – *armchair* (7,7), *2* – *zigzag* (12,0), *3* – *zigzag* (19,0) (the views along the tubes' axis are shown) and *4* – a diagonal view for *zigzag* (19,0) NT. Different colors show equipotential surfaces: -3.0, -2.0, -1.0, 1.0, 2.0 and 3.0 e/Å. Reprinted with permission from(Guimaraes *et al.*, 2010). Copyright 2010 American Chemical Society.

Experimental results from natural samples indicate that the halloysite structure at the edge is disrupted, and the surface groups can be protonated or deprotonated originating variable charge (Theng *et al.*, 1982). For instance, halloysite presents negative charge at pH higher than 3 (Theng *et al.*, 1982), and its isoelectric point is around pH 3. In this way, the edges are considered to be positively charged at low pH, neutral at isoeletric point and negatively charged at higher pH (Braggs *et al.*, 1994). The negative charge can be ascribed to the deprotonation of water and hydroxyl groups bound to aluminum and silicon at the edges (Theng *et al.*, 1982), and the hydroxyl groups are considered to be the principal reactive sites. Furthermore, Machado *et al.* (2008) have shown the immobilization of anionic and cationic metalloporphyrins into halloysite NTs occurs at high rates while for neutral metalloporphyrins the immobilization was not observed. The cationic immobilization can occur via SiO^- groups, while anionic immobilization may occur through aluminol groups at halloysite edges.

5. Chrysotile nanotubes – Structural properties

Chrysotile and lizardite are fibrous natural phylosilicate minerals which belong to the serpentine group and present 1:1 structure. They have the same empirical formula $Mg_3Si_2O_5(OH)_4$ (Falini *et al.*, 2004; Anbalagan *et al.*, 2010), as can be seen in figure 10. Chrysotile constitutes approximately 95% percent of the manufactured asbestos and presents three polytypes: clinochrysotile (Whittaker, 1956a), orthochrysotile (Whittaker, 1956b) and parachrysotile (Whittaker, 1956c). Clinochrysotile is the most common one. While lizardite, more abundant than chrysotile, presents a planar shape, chrysotile presents a tubular form. Chrysotile and lizardite are composed by octahedral sheet, brucite

(magnesium dihydroxide, $Mg(OH)_2$) and tetrahedral layer tridymite (silicon dioxide, SiO_2), figure 10. The outer part of chrysotile is formed by brucite and the inner part by tridymite.

Figure 10 shows the structures of tridymite, brucite, lizardite and chrysotile. The superposition of the tetrahedral and octahedral layers results in 1:1 lizardite which has the hexagons formed by Mg-O bounds (from brucite) located on the center of the hexagon formed by Si-O bounds (from tridymite). The connections of brucite and tridymite to form lizardite occur via the apical oxygen of the SiO_4 layer which are connected directly with the Mg atoms of brucite. The connection of brucite and tridymite layers occurs in the same way as in chrysotile NTs.

Chrysotile is a nanosized and tube-shaped material with lower mechanical strength and it is always uncapped. Chrysotile (Piperno *et al.*, 2007; Anbalagan *et al.*, 2010) can be synthesized in aqueous solution under mild conditions, easily modified (Wypych *et al.*, 2004; Wang *et al.*, 2006; Wang *et al.*, 2009) and functionalized (Nakagaki & Wypych, 2007). Therefore chrysotile is an interesting target material to be used as component of hybrid materials, support for catalysis, ionic channels, molecular sieving, for gas storage (Halma *et al.*, 2006; Nakagaki *et al.*, 2006; Nakagaki & Wypych, 2007) and other applications in nanotechnology. Stoichiometric chrysotile has been synthesized and characterized by structural and spectroscopy analyses (Falini *et al.*, 2002; Falini *et al.*, 2004). Chrysotile is found as multiwalled nanotubes with inner diameter around 1-10 nm, outer diameter around 10-50 nm and the size can reach the millimeter range (Falini *et al.*, 2004). Chrysotile can also be found in spiral form (Yada, 1967, 1971).

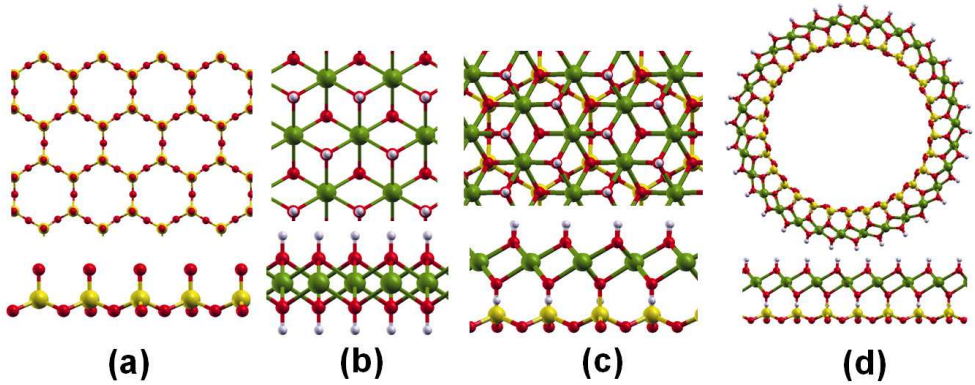

Fig. 10. Top view and side view of (a) tridymite (SiO_2), (b) brucite ($Mg(OH)_2$), c) lizardite ($Mg_3Si_2O_5(OH)_4$) layers and (d) chrysotile NT. Atoms label: Si, yellow; O, red; H, white; Mg, green.

Chrysotile NTs were synthesized and characterized by Piperno and co-workers (2007) using atomic force microscopy and transmission electron Microscopy (TEM). The results have shown that chrysotile NTs exhibit elastic behavior at small deformation. The chrysotile Young's modulus evaluated by (Piperno *et al.*, 2007) are 159 ± 125 GPa. The stoichiometric chrysotile fibers demonstrate a hollow structure with quite uniform outer diameter around 35 nm and inner diameter about 7-8 nm. The NTs are open ended with several hundred nanometers in length.

Only few theoretical studies concerning chrysotile NTs have been carried out. The chrysotile unit cell is composed by hundreds up to thousands of atoms and, therefore, DFT or *ab initio* calculations on such systems are computationally time consuming. D'Arco *et al.* (2009) have studied the stability and structural properties of some armchair chrysotile NTs using the DFT method and helical symmetry approach as it is implemented in the CRYSTAL program (Dovesi *et al.*, 2009). The structural results are in good agreement with the experimental data for NTs and lizardite monolayer. Preliminary results of the strain energy curve of chrysotile calculated using the SCC-DFTB method decreases monotonically with the increase of the radii indicating the monolayer is more stable than the NTs. The chirality does not affect the relative stability of the NTs, i.e., strain energy profile for *zigzag* and *armchair* NTs present the same pattern. In spite of the polydispersity of the chrysotile NTs and the environmental concern of asbestos, many attempts for modifying and functionalizing chrysotile NTs have been reported. Chrysotile has been studied in many fields such as support for immobilization of metalloporphyrins, oxidation catalysts, fixation of CO_2 by chrysotile under low-pressure (Larachi *et al.*, 2010), modification of chrysotile surface by organosilanes, functionalization of single layers and nanofibers to produce polymer nanocomposites (Wang *et al.*, 2006; Nakagaki & Wypych, 2007; Wang *et al.*, 2009) and to produce self-assembled systems (De Luca *et al.*, 2009). Furthermore, many studies have reported the partial or total substitutions of magnesium atoms at chrysotile sites for different atoms as Fe and Ni (Bloise *et al.*, 2010). The substitution of Mg atoms at chrysotile by Ni results in another nanotubular material called pecorite (Faust *et al.*, 1969) with empirical formula $Ni_3Si_2O_5(OH)_4$ similar to that of chrysotile. Pecorite and its planar form (called nepouite) can be found in nature (Faust *et al.*, 1969) or synthesized (McDonald *et al.*, 2009; Bloise *et al.*, 2010). Since nickel atoms are usually applied in catalysis, Ni-containing phyllosilicates (Ni-lizardite or nepouite) have been used as catalysts precursors for carbon dioxide reforming of methane (Sivaiah *et al.*, 2011).

The acid leaching of chrysotile is a process used to synthesize SiO_2 nano tubular structure which has been reported recently (Wang *et al.*, 2006). The process occurs by leaching of brucite layers and the reminiscent product is an amorphous material called nano-fibriform silica (Wang *et al.*, 2006) which presents tubular shape and the diameter around 20-30 nm. SCC-DFTB calculations of SiO_2 NTs indicate that these structures are not stable and may easily collapse to the silica structure. However, it opens an interesting opportunity to functionalize the NT surface and eventually create a carbon based structure surrounding the tridymite, SiO_2, structure. Actually, Wang *et al.* (2009) have been able to modify the outer surface of the nano-fibriform silica with dimethyldichorosilane. Theoretical investigations of these recently synthesized systems can bring important insights about their structural and mechanical properties and eventually indicate the possibility to design materials with enhanced properties.

6. Final remarks

Nanostructured aluminosilicates are becoming the target for new advanced materials. Their availability, the syntheses in mild conditions and their well defined structures are very attractive characteristics. They are easily functionalized and much effort has been devoted to modify their structures and to enhance their physical and chemical properties. Particularly, the aluminosilicate nanostructure can be envisaged for the development of nanoreactors,

controlled release devices, ion conductors for batteries, gas storage and separation systems. They are insulator and the stiffness of the NT is similar to other inorganic NTs and comparable to steel. Much progress in characterizing and developing new materials based on clay mineral NTs has been obtained in the last few years. The modification (Kang *et al*., 2010) and the functionalization (Kang *et al*., 2011) of the imogolite NTs inner walls are recent notable achievements that open new perspectives on the field. Understanding the formation mechanism of such nanostructured clay minerals is also an important achievement broadening the fundamental knowledge about clay mineral NTs. The synthesis of new imogolite-like structures is an important issue and deserves more attention. Actually, the aluminogermanate NTs (Levard *et al*., 2008; Levard *et al*., 2010) are an important example of the feasibility of this task and more effort in this direction must be done. In fact, lamellar gibbsite can be seen as a template for modeling and synthesizing new nanostructured imogolite-like structures. Actually, the use of clay NTs for developing new advanced materials has not yet received much attention commensurate with their potential for technological application.

7. Acknowledgments

Support from the agencies Fundação de Amparo à Pesquisa de Minas Gerais (FAPEMIG), Coordenação de Aperfeiçoamento de Pessoal de Nível Superior (CAPES), and Conselho Nacional para o Desenvolvimento Científico e Tecnológico (CNPq), Deutsche Forschungsgemeinschaft (DFG) and Deutscher Akademischer Auslandsdienst (DAAD) are gratefully acknowledged. This work has also been supported by the Brazilian Initiative National Institute of Science and Technology for Mineral Resources, Water and Biodiversity, INCT-ACQUA.

8. References

Ackerman, W.C., Smith, D.M., Huling, J.C., Kim, Y.W., Bailey, J.K. & Brinker, C.J. (1993) Gas vapor adsorption in imogolite - a microporous tubular aluminosilicate. *Langmuir*, 9, 1051-1057.

Alvarez-Ramirez, F. (2007) Ab initio simulation of the structural and electronic properties of aluminosilicate and aluminogermanate natotubes with imogolite-like structure. *Physical Review B*, 76.

Anbalagan, G., Sivakumar, G., Prabakaran, A.R. & Gunasekaran, S. (2010) Spectroscopic characterization of natural chrysotile. *Vibrational Spectroscopy*, 52, 122-127.

Aradi, B., Hourahine, B. & Frauenheim, T. (2007) Dftb+, a sparse matrix-based implementation of the dftb method. *Journal of Physical Chemistry A*, 111, 5678-5684.

Artacho, E., Sanchez-Portal, D., Ordejon, P., Garcia, A. & Soler, J.M. (1999) Linear-scaling ab-initio calculations for large and complex systems. *Physica Status Solidi B-Basic Research*, 215, 809-817.

Bates, T.F., Hildebrand, F.A. & Swineford, A. (1950a) Morphology and structure of endellite and halloysite. *American Mineralogist*, 35, 463-484.

Bates, T.F., Sand, L.B. & Mink, J.F. (1950b) Tubular crystals of chrysotile asbestos. *Science*, 111, 512-513.

Bi, S.P., Wang, C.Y., Cao, Q. & Zhang, C.H. (2004) Studies on the mechanism of hydrolysis and polymerization of aluminum salts in aqueous solution: Correlations between the "core-links" model and "cage-like" keggin-al-13 model. *Coordination Chemistry Reviews*, 248, 441-455.

Bloise, A., Belluso, E., Fornero, E., Rinaudo, C., Barrese, E. & Capella, S. (2010) Influence of synthesis conditions on growth of ni-doped chrysotile. *Microporous and Mesoporous Materials*, 132, 239-245.

Braggs, B., Fornasiero, D., Ralston, J. & Stsmart, R. (1994) The effect of surface modification by an organosilane on the electrochemical properties of kaolinite. *Clays and Clay Minerals*, 42, 123-136.

Bursill, L.A., Peng, J.L. & Bourgeois, L.N. (2000) Imogolite: An aluminosilicate nanotube material. *Philosophical Magazine A, Physics of Condensed Matter Structure Defects and Mechanical Properties*, 80, 105-117.

Casey, W.H. (2006) Large aqueous aluminum hydroxide molecules. *Chemical Reviews*, 106, 1-16.

Cradwick, P.D., Wada, K., Russell, J.D., Yoshinag.N, Masson, C.R. & Farmer, V.C. (1972) Imogolite, a hydrated aluminum silicate of tubular structure. *Nature-Physical Science*, 240, 187-&.

D'Arco, P., Noel, Y., Demichelis, R. & Dovesi, R. (2009) Single-layered chrysotile nanotubes: A quantum mechanical ab initio simulation. *Journal of Chemical Physics*, 131.

De Luca, G., Romeo, A., Villari, V., Micali, N., Foltran, I., Foresti, E., Lesci, I.G., Roveri, N., Zuccheri, T. & Scolaro, L.M. (2009) Self-organizing functional materials via ionic self assembly: Porphyrins h- and j-aggregates on synthetic chrysotile nanotubes. *Journal of the American Chemical Society*, 131, 6920-6921.

Demichelis, R., Noel, Y., D'Arco, P., Maschio, L., Orlando, R. & Dovesi, R. (2010) Structure and energetics of imogolite: A quantum mechanical ab initio study with b3lyp hybrid functional. *Journal of Materials Chemistry*, 20, 10417-10425.

Dixon, J.B. & McKee, T.R. (1974) Internal and external morphology of tubular and spheroidal halloysite particles. *Clays and Clay Minerals*, 22, 127-137.

Doucet, F.J., Schneider, C., Bones, S.J., Kretchmer, A., Moss, I., Tekely, P. & Exley, C. (2001) The formation of hydroxyaluminosilicates of geochemical and biological significance. *Geochimica Et Cosmochimica Acta*, 65, 2461-2467.

Dovesi, R., Saunders, V.R., Roetti, C., Orlando, R., Zicovich-Wilson, C.M., Pascale, F., Civalleri, B., Doll, K., Harrison, N.M., Bush, I.J., D'Arco, P. & Llunell, M. (2009) Crystal09 user's manual. Pp.,University of Torino, Torino.

Dresselhaus, M.S., Dresselhaus, G. & Avouris, P. (2001) Carbon nanotubes: Synthesis, structure, properties and applications. Pp. *Topics in applied physics*, 80,Springer-Verlag, Berlin Heidelberg.

Elstner, M., Porezag, D., Jungnickel, G., Elsner, J., Haugk, M., Frauenheim, T., Suhai, S. & Seifert, G. (1998) Self-consistent-charge density-functional tight-binding method for simulations of complex materials properties. *Physical Review B*, 58, 7260-7268.

Endo, M., Iijima, S. & Dresselhaus, M.S. (1996) Carbon nanotubes. Pp.,Pergamon.

Enyashin, A.N. & Seifert, G. (2005) Structure, stability and electronic properties of TiO_2 nanostructures. *Physica Status Solidi B-Basic Solid State Physics*, 242, 1361-1370.

Enyashin, A.N., Gemming, S. & Seifert, G. (2007) Simulation of inorganic nanotubes. Pp. 33-57. In S. Gemming, M. Schreiber, and J.-B. Suck, Eds. *Materials for tomorrow*, 93,Springer Berlin Heidelberg.

Enyashin, A.N. & Ivanovskii, A.L. (2008) Theoretical prediction of al(oh)(3) nanotubes and their properties. *Physica E-Low-Dimensional Systems & Nanostructures*, 41, 320-323.

Enyashin, A.N., Popov, I. & Seifert, G. (2009) Stability and electronic properties of rhenium sulfide nanotubes. *Physica Status Solidi B-Basic Solid State Physics*, 246, 114-118.

Exley, C., Schneider, C. & Doucet, F.J. (2002) The reaction of aluminium with silicic acid in acidic solution: An important mechanism in controlling the biological availability of aluminium? *Coordination Chemistry Reviews*, 228, 127-135.

Falini, G., Foresti, E., Gazzano, M., Gualtieri, A.E., Leoni, M., Lesci, I.G. & Roveri, N. (2004) Tubular-shaped stoichiometric chrysotile nanocrystals. *Chemistry-A European Journal*, 10, 3043-3049.

Falini, G., Foresti, E., Lesci, G. & Roveri, N. (2002) Structural and morphological characterization of synthetic chrysotile single crystals. *Chemical Communications*, 1512-1513.

Faust, G.T., Fahey, J.J., Mason, B. & Dwornik, E.J. (1969) Pecoraite, ni6si4o10(oh)8, nickel analog of clinochrysotile, formed in the wolf creek meteorite. *Science*, 165, 59-60.

Frenzel, J., Oliveira, A.F., Duarte, H.A., Heine, T. & Seifert, G. (2005) Structural and electronic properties of bulk gibbsite and gibbsite surfaces. *Zeitschrift Fur Anorganische Und Allgemeine Chemie*, 631, 1267-1271.

Giese, R.F. & Datta, P. (1973) Hydroxyl orientation in kaolinite, dickite, and nacrite *American Mineralogist*, 58, 471-479.

Guimaraes, L., Enyashin, A.N., Frenzel, J., Heine, T., Duarte, H.A. & Seifert, G. (2007) Imogolite nanotubes: Stability, electronic, and mechanical properties. *ACS Nano*, 1, 362-368.

Guimaraes, L., Enyashin, A.N., Seifert, G. & Duarte, H.A. (2010) Structural, electronic, and mechanical properties of single-walled halloysite nanotube models. *Journal of Physical Chemistry C*, 114, 11358-11363.

Halma, M., Bail, A., Wypych, F. & Nakagaki, S. (2006) Catalytic activity of anionic iron(iii) porphyrins immobilized on grafted disordered silica obtained from acidic leached chrysotile. *Journal of Molecular Catalysis A-Chemical*, 243, 44-51.

Hedicke-Höchstötter, K., Lim, G.T. & Altstädt, V. (2009) Novel polyamide nanocomposites based on silicate nanotubes of the mineral halloysite. *Composites Science and Technology*, 69, 330-334.

Heine, T., Rapacioli, M., Patchkovskii, S., Frenzel, J., Koester, A.M., Calaminici, P., Escalante, S., Duarte, H.A., Flores, R., Geudtner, G., Goursot, A., Reveles, J.U., Vela, A. & Salahub, D.R. (2009) Demon, demon-nano edn. Pp.,deMon-Sofware, Mexico, Bremen.

Hernandez, E., Goze, C., Bernier, P. & Rubio, A. (1998) Elastic properties of c and bxcynz composite nanotubes. *Physical Review Letters*, 80, 4502-4505.

Iijima, S. (1991) Helical microtubules of graphitic carbon. *Nature (London)*, 354 56.

Imamura, S., Kokubu, T., Yamashita, T., Okamoto, Y., Kajiwara, K. & Kanai, H. (1996) Shape-selective copper-loaded imogolite catalyst. *Journal of Catalysis*, 160, 137-139.

Ivanovskaya, V.V., Heine, T., Gemming, S. & Seifert, G. (2006) Structure, stability and electronic properties of composite mo1-xnbxs2 nanotubes. *Physica Status Solidi B-Basic Solid State Physics*, 243, 1757-1764.

Joussein, E., Petit, S., Churchman, J., Theng, B., Righi, D. & Delvaux, B. (2005) Halloysite clay minerals - a review. *Clay Minerals*, 40, 383-426.

Kang, D.Y., Zang, J., Jones, C.W. & Nair, S. (2011) Single-walled aluminosilicate nanotubes with organic-modified interiors. *Journal of Physical Chemistry C*, 115, 7676-7685.

Kang, D.Y., Zang, J., Wright, E.R., McCanna, A.L., Jones, C.W. & Nair, S. (2010) Dehydration, dehydroxylation, and rehydroxylation of single-walled aluminosilicate nanotubes. *Acs Nano*, 4, 4897-4907.

Kelly, H.M., Deasy, P.B., Ziaka, E. & Claffey, N. (2004) Formulation and preliminary in vivo dog studies of a novel drug delivery system for the treatment of periodontitis. *International Journal of Pharmaceutics*, 274, 167-183.

Konduri, S., Mukherjee, S. & Nair, S. (2006) Strain energy minimum and vibrational properties of single-walled aluminosilicate nanotubes. *Physical Review B*, 74, 033401.

Kuc, A. & Heine, T. (2009) Shielding nanowires and nanotubes with imogolite: A route to nanocables. *Advanced Materials*, 21, 4353-+.

Larachi, F., Daldoul, I. & Beaudoin, G. (2010) Fixation of co2 by chrysotile in low-pressure dry and moist carbonation: Ex-situ and in-situ characterizations. *Geochimica et Cosmochimica Acta*, 74, 3051-3075.

Lee, S.U., Choi, Y.C., Youm, S.G. & Sohn, D. (2011) Origin of the strain energy minimum in imogolite nanotubes. *Journal of Physical Chemistry C*, 115, 5226-5231.

Levard, C., Rose, J., Masion, A., Doelsch, E., Borschneck, D., Olivi, L., Dominici, C., Grauby, O., Woicik, J.C. & Bottero, J.-Y. (2008) Synthesis of large quantities of single-walled aluminogermanate nanotube. *Journal of the American Chemical Society*, 130, 5862-+.

Levard, C., Rose, J., Thill, A., Masion, A., Doelsch, E., Maillet, P., Spalla, O., Olivi, L., Cognigni, A., Ziarelli, F. & Bottero, J.Y. (2010) Formation and growth mechanisms of imogolite-like aluminogermanate nanotubes. *Chemistry Of Materials*, 22, 2466-2473.

Levis, S.R. & Deasy, P.B. (2003) Use of coated microtubular halloysite for the sustained release of diltiazem hydrochloride and propranolol hydrochloride. *International Journal of Pharmaceutics*, 253, 145-157.

Liu, R., Zhang, B., Mei, D., Zhang, H. & Liu, J. (2011) Adsorption of methyl violet from aqueous solution by halloysite nanotubes. *Desalination*, 268, 111-116.

Lvov, Y.M., Shchukin, D.G., Mohwald, H. & Price, R.R. (2008) Halloysite clay nanotubes for controlled release of protective agents. *Acs Nano*, 2, 814-820.

Machado, G.S., Castro, K., Wypych, F. & Nakagaki, S. (2008) Immobilization of metalloporphyrins into nanotubes of natural halloysite toward selective catalysts for oxidation reactions. *Journal of Molecular Catalysis a-Chemical*, 283, 99-107.

McDonald, A., Scott, B. & Villemure, G. (2009) Hydrothermal preparation of nanotubular particles of a 1:1 nickel phyllosilicate. *Microporous and Mesoporous Materials*, 120, 263-266.

Mukherjee, S., Bartlow, V.A. & Nair, S. (2005) Phenomenology of the growth of single-walled aluminosilicate and aluminogermanate nanotubes of precise dimensions. *Chemistry Of Materials*, 17, 4900-4909.

Nakagaki, S., Castro, K., Machado, G.S., Halma, M., Drechsel, S.M. & Wypych, F. (2006) Catalytic activity in oxidation reactions of anionic iron(iii) porphyrins immobilized on raw and grafted chrysotile. *Journal of the Brazilian Chemical Society*, 17, 1672-1678.

Nakagaki, S. & Wypych, F. (2007) Nanofibrous and nanotubular supports for the immobilization of metalloporphyrins as oxidation catalysts. *Journal of Colloid and Interface Science*, 315, 142-157.

Oliveira, A.F., Seifert, G., Heine, T. & Duarte, H.A. (2009) Density-functional based tight-binding: An approximate dft method. *Journal of the Brazilian Chemical Society*, 20, 1193-1205.

Pauling, L. (1930) The structure of the chlorites. *Proceedings of the National Academy of Sciences of the United States of America*, 16, 578-582.

Piperno, S., Kaplan-Ashiri, I., Cohen, S.R., Popovitz-Biro, R., Wagner, H.D., Tenne, R., Foresti, E., Lesci, I.G. & Roveri, N. (2007) Characterization of geoinspired and synthetic chrysotile nanotubes by atomic force microscopy and transmission electron microscopy. *Advanced Functional Materials*, 17, 3332-3338.

Price, R. & Gaber, B. Controled release of active agents using inorganic tubules. Pp.,5651976, US Patent.

Price, R.R., Gaber, B.P. & Lvov, Y.M. (2001) In-vitro release characteristics of tetracycline hcl, khellin and nicotinamide adenine dineculeotide from halloysite; a cylindrical mineral. *Journal of Microencapsulation*, 18, 713.

Rasche, B., Seifert, G. & Enyashin, A. (2010) Stability and electronic properties of bismuth nanotubes. *Journal of Physical Chemistry C*, 114, 22092-22097.

Redlinger, M. & Corkery, R. (2007) Cosmetic skincare applications employing mineral derived tubules for controlled release. Pp.,0202061, US Patent.

Remskar, M. (2004) Inorganic nanotubes. *Advanced Materials*, 16, 1497-1504.

Schneider, C., Doucet, F., Strekopytov, S. & Exley, C. (2004) The solubility of an hydroxyaluminosilicate. *Polyhedron*, 23, 3185-3191.

Seifert, G., Terrones, H., Terrones, M., Jungnickel, G. & Frauenheim, T. (2000) Structure and electronic properties of mos2 nanotubes. *Physical Review Letters*, 85, 146-149.

Shchukin, D.G. & Mohwald, H. (2007) Surface-engineered nanocontainers for entrapment of corrosion inhibitors. *Advanced Functional Materials*, 17, 1451-1458.

Shchukin, D.G., Sukhorukov, G.B., Price, R.R. & Lvov, Y.M. (2005) Halloysite nanotubes as biomimetic nanoreactors. *Small*, 1, 510-513.

Shchukin, D.G., Zheludkevich, M., Yasakau, K., Lamaka, S., Ferreira, M.G.S. & Mohwald, H. (2006) Layer-by-layer assembled nanocontainers for self-healing corrosion protection. *Advanced Materials*, 18, 1672-+.

Sivaiah, M.V., Petit, S., Beaufort, M.F., Eyidi, D., Barrault, J., Batiot-Dupeyrat, C. & Valange, S. (2011) Nickel based catalysts derived from hydrothermally synthesized 1:1 and 2:1 phyllosilicates as precursors for carbon dioxide reforming of methane. *Microporous and Mesoporous Materials*, 140, 69-80.

Soler, J.M., Artacho, E., Gale, J.D., Garcia, A., Junquera, J., Ordejon, P. & Sanchez-Portal, D. (2002) The siesta method for ab initio order-n materials simulation. *Journal of Physics-Condensed Matter*, 14, 2745-2779.

Stefanov, M., Enyashin, A.N., Heine, T. & Seifert, G. (2008) Nanolubrication: How do mos2-based nanostructures lubricate? *Journal of Physical Chemistry C*, 112, 17764-17767.

Tamura, K. & Kawamura, K. (2002) Molecular dynamics modeling of tubular aluminum silicate: Imogolite. *Journal of Physical Chemisty B*, 106, 271-278.

Tenne, R. (2006) Inorganic nanotubes and fullerene-like nanoparticles. *Nature Nanotechnology*, 1, 103-111.

Tenne, R., Margulis, L., Genut, M. & Hodes, G. (1992) Polyhedral and cylindrical structures of tungsten disulfide. *Nature*, 360, 444-446.

Theng, B.K.G., Russell, M., Churchman, G.J. & Parfitt, R.L. (1982) Surface-properties of allophane, halloysite, and imogolite. *Clays and Clay Minerals*, 30, 143-149.

Veerabadran, N.G., Price, R.R. & Lvov, Y.M. (2007) Clay nanotubes for encapsulation and sustained release of drugs. *Nano*, 2, 115-120.

Wang, L.J., Lu, A.H., Wang, C.Q., Zheng, X.S., Zhao, D.J. & Liu, R. (2006) Nano-fibriform production of silica from natural chrysotile. *Journal of Colloid and Interface Science*, 295, 436-439.

Wang, L.J., Lu, A.H., Xiao, Z.Y., Ma, J.H. & Li, Y.Y. (2009) Modification of nano-fibriform silica by dimethyldichlorosilane. *Applied Surface Science*, 255, 7542-7546.

White, C.E., Provis, J.L., Riley, D.P., Kearley, G.J. & van Deventer, J.S.J. (2009) What is the structure of kaolinite? Reconciling theory and experiment. *Journal of Physical Chemistry B*, 113, 6756-6765.

Whittaker, E.J.W. (1956a) The structure of chrysotile .2. Clino-chrysotile. *Acta Crystallographica*, 9, 855-862.

Whittaker, E.J.W. (1956b) The structure of chrysotile .3. Ortho-chrysotile. *Acta Crystallographica*, 9, 862-864.

Whittaker, E.J.W. (1956c) The structure of chrysotile .4. Para-chrysotile. *Acta Crystallographica*, 9, 865-867.

Wypych, F., Schreiner, W.H. & Richard, E. (2004) Grafting of phenylarsonic and 2-nitrophenol-4-arsonic acid onto disordered silica obtained by selective leaching of brucite-like sheet from chrysotile structure. *Journal of Colloid and Interface Science*, 276, 167-173.

Yada, K. (1967) Study of chrysotile asbestos by a high resolution electron microscope. *Acta Crystallographica*, 23, 704-&.

Yada, K. (1971) Study of microstructure of chrysotile asbestos by high resolution electron microscopy. *Acta Crystallographica Section a-Crystal Physics Diffraction Theoretical and General Crystallography*, A 27, 659-&.

Yucelen, G.I., Choudhury, R.P., Vyalikh, A., Scheler, U., Beckham, H.W. & Nair, S. (2011) Formation of single-walled aluminosilicate nanotubes from molecular precursors and curved nanoscale intermediates. *Journal of the American Chemical Society*, 133, 5397-5412.

Zhao, M.W., Xia, Y.Y. & Mei, L.M. (2009) Energetic minimum structures of imogolite nanotubes: A first-principles prediction. *Journal of Physical Chemistry C*, 113, 14834-14837.

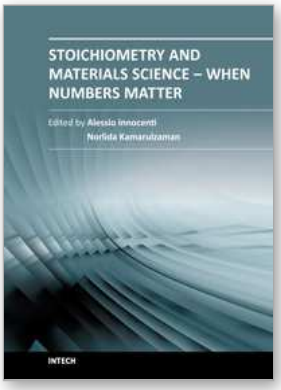

Stoichiometry and Materials Science - When Numbers Matter
Edited by Dr. Alessio Innocenti

ISBN 978-953-51-0512-1
Hard cover, 436 pages
Publisher InTech
Published online 11, April, 2012
Published in print edition April, 2012

The aim of this book is to provide an overview on the importance of stoichiometry in the materials science field. It presents a collection of selected research articles and reviews providing up-to-date information related to stoichiometry at various levels. Being materials science an interdisciplinary area, the book has been divided in multiple sections, each for a specific field of applications. The first two sections introduce the role of stoichiometry in nanotechnology and defect chemistry, providing examples of state-of-the-art technologies. Section three and four are focused on intermetallic compounds and metal oxides. Section five describes the importance of stoichiometry in electrochemical applications. In section six new strategies for solid phase synthesis are reported, while a cross sectional approach to the influence of stoichiometry in energy production is the topic of the last section. Though specifically addressed to readers with a background in physical science, I believe this book will be of interest to researchers working in materials science, engineering and technology.

InTech Europe
University Campus STeP Ri
Slavka Krautzeka 83/A
51000 Rijeka, Croatia
Phone: +385 (51) 770 447
Fax: +385 (51) 686 166
www.intechopen.com

InTech China
Unit 405, Office Block, Hotel Equatorial Shanghai
No.65, Yan An Road (West), Shanghai, 200040, China
中国上海市延安西路65号上海国际贵都大饭店办公楼405单元
Phone: +86-21-62489820
Fax: +86-21-62489821